Reconfigurable Intelligent Surface-Assisted RF Wireless Power Transfer for Internet of Things System: Modeling and Evaluation

Arif Abdul Aziz[1]*, Istiqomah[2], Fiky Y. Suratman[3]
[1,2,3] Department of Electrical Engineering, Telkom University, Indonesia
[1,2,3] University Center of Excellence for Intelligent Sensing-IoT , Telkom University, Indonesia
[1,2,3] Kabupaten Bandung, Jawa Barat, Indonesia 40257
*Email : [1]arifabdulaziz@telkomuniversity.ac.id

ARTICLE INFORMATION

Received on 08 May 2024
Revised on 10 June 2024
Accepted on 21 June 2024

Keywords:
Internet of Things
Metasurface
Multiple Input Single Output (MISO)
Reconfigurable Intelligent Surface
RF Wireless Power Transfer

ABSTRACT

This work studies the utilization of reconfigurable intelligent surfaces (RIS) for assisting radiofrequency (RF)-based wireless power transfer (WPT) in the Internet of Things (IoT) system. The RIS device in this system is utilized to provide the line of sight (LOS) path when an obstacle blocks the direct power transmission from the transmitter to the receiver. This work presents a comprehensive modeling of the RIS-assisted RF WPT for IoT systems, which includes the spatial model, the RIS-assisted RF WPT model, and the total receiver power model. The performance of RIS-assisted RF WPT is evaluated by simulation matched to the IoT system. In all simulation tests, the obstacle is located between the transmission and the receiver, eliminating direct power transfer. By simulation, it has been verified that the RIS device can assist the RF WPT in the IoT system. The receiver can achieve 0,4714% power transfer efficiency at a distance of 1 meter from the RIS device. Meanwhile, 0,0290% power transfer efficiency is achieved within a 15-meter distance from the RIS device. Furthermore, the performance of RIS-assisted RF WPT with various numbers of unit cells in the RF WPT system is investigated. It has been found that increasing the number of unit cells in RF WPT after a certain number is ineffective for the RF WPT in an IoT system.

1. Introduction

Radiofrequency (RF)-based wireless power transfer (WPT) is a radiative wireless power technology that utilizes electromagnetic (EM) waves to transfer energy wirelessly. RF WPT technology can operate much farther than non-radiative technology, such as magnetic resonance and resonant inductive coupling. Unfortunately, with such an advantage over other systems, the RF WPT technology can only achieve low power transfer efficiency (Lu et al., 2015). Thus, the best application of the RF WPT technology is for a system that consumes low power, such as the Internet of Things (IoT) system (Xie et al., 2013).

The implementation of RF WPT technology in the IoT system comes with many challenges. To maintain effective power transfer, the RF WPT must be performed by line of sight (LOS) without any obstacle between the radiation path of the transmitter and receiver antenna. Even though the EM signal can penetrate objects, the EM signal will be significantly attenuated after penetrating particular objects (Taylor et al., 1997, 1999). In this case, the received power is further reduced, and the power transfer efficiency becomes tiny and unusable for the IoT device. Therefore, we need to find a solution for the obstacle problem in the RF WPT system.

To enable the 6th-generation mobile network, many researchers have developed a novel antenna technology called reconfigurable intelligent surface (RIS) (Pan et al., 2021). This novel antenna technology is introduced as a mirror-like device that can create an alternative channel path between two communication devices when the direct LOS between these devices is not present (Wu & Zhang, 2020). Basically, the concept and working

DOI: doi.org/10.17933/bpostel.v22i1.396

principle of the RIS are similar to those of the metasurface. Both devices utilize an antenna array to reflect the incoming signal as a concentrated reflected beam toward the desired location. The RIS device is introduced as a metasurface that can be actively configured via software. This feature allows the RIS device to actively control the amplitude, phase, and polarization of the reflected signal in order to reconfigure the wireless propagation environment (Selvaraj et al., 2023).

Typically, the RIS device consists of numerous reflected antenna elements, where each reflected antenna is called a unit cell. In RIS, each unit cell can be independently controlled to manipulate the incoming EM wave (Gong et al., 2020). With this capability, when the EM signal is radiated toward the RIS device, the RIS device can control the direction of the reflected signal. Thus, the reflected signal can be formed as a beam focused toward the location of the receiver (Yang et al., 2016). Henceforth, with the assistance of the RIS device, data or wireless power from the transmitter can be transferred to the receiver without the direct LOS propagation path available between both devices.

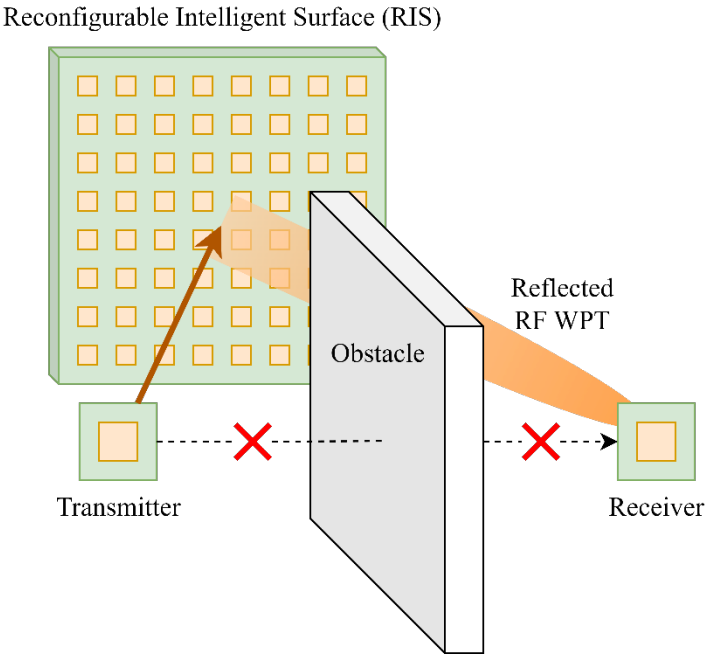

Figure 1. Reconfigurable Intelligent Surface-Assisted RF Wireless Power Transfer System

As shown in Figure 1, this paper studies the RIS-assisted RF WPT system that provides an alternative propagation path, especially when an obstacle is blocking the direct LOS channel between two WPT devices. Through this system, the RF WPT emitted from the transmitter device is received and then re-radiated by the RIS as a reflected beam signal toward the receiver. Therefore, the receiver can optimally receive the EM signal even though the obstacle blocks the direct LOS channel. This study provides a comprehensive RIS-assisted RF WPT system model, including the spatial and EM propagation models. The performance evaluation of RIS configurations is analyzed for the RF WPT, especially for the IoT system.

The remainder of this journal is organized as follows: The literature review of the RIS-assisted RF WPT system is presented in Section 2. The system model of RIS-assisted RF WPT is described in Section 3. Section 4 presents the simulation parameters of the RIS-assisted RF WPT system. The performance evaluation of the RIS-assisted RF WPT system is given in Section 5. Section 6 concludes this study.

2. Literature review

The first concept of WPT was introduced by Nikola Tesla in the 19th century. Since then, researchers have attempted to develop and implement the WPT in many areas, especially in IoT systems. In 2018, Rana et al. (2018) introduced the IoT infrastructure for the WPT system. A state-space model of WPT for IoT systems and the innovative IoT-based communication infrastructure is presented in their study. The proposed system works much better than the existing methods. Nusrat et al. (2023) demonstrate a complete end-to-end WPT system at 2.4 GHz. Their system consists of a 2×4 antenna array that transmits 5 dBm and 15 dBm of power. At a 20-cm distance, the receiver receives -29.38 dBm of power when the transmitter is transmitting power at 15 dBm. Cha et al. (2018) study simultaneous wireless information and power transfer (SWIPT) for IoT systems by proposing a novel strategy for SWIPT transmission. Their system significantly improves SWIPT performance compared to other related work. Other work demonstrates that the RF WPT can be used along with different technologies, such as drones, to deliver power in close proximity to the IoT device that is out of the scope of the power beacon. By utilizing the RF WPT from the drone, the IoT device performs a beam-rotation forward scatter algorithm to send information to the base station (Aziz et al., 2022). Meanwhile, Choi et al. (2019) have demonstrated that using a massive-phase antenna array system can extend the range of RF WPT for IoT systems. This work shows that the RF WPT from the power beacon can operate a battery-less IoT device located 50 meters from the power beacon. The battery-less IoT device that has been tested can survive only with the power from the WPT for up to 20 minutes without draining stored power from the supercapacitor.

Sahu (2014) studied the RF propagation losses while penetrating homogenous brick and concrete walls. In their study, RF signals from 1 to 5 GHz are set to penetrate 20-cm walls. Their research shows that 20-cm walls introduce transmission loss from 2 dB to 10 dB to the RF signal while penetrating the walls. Another study shows the effects of common materials such as cardboard, plastic, liquids, metals, and other materials on the RF signal. This study shows that certain materials can absorb, detune, and reflect the RF signal that is radiated to them (Keskilammi, 2004).

Many studies have attempted to utilize the RIS system for the WPT. Tran et al. (2022b) implemented a 16×16-unit cell RIS system for WPT. Each unit cell is a 1-bit unit cell that can modify the reflected signal by a 180-degree phase difference at each bit stage. This system is used in the multiple-input multiple-output (MIMO) WPT system operating at 5.8 GHz. This work is then extended to simultaneously charge multiple devices using the RIS system (Tran et al., 2022a). Another study also shows the RIS system can serve multiusers by envelope beamforming for WPT (Yang et al., 2021). Meanwhile, Mohjazi et al. (2022) propose the battery recharging time model for RIS-assisted WPT. The proposed system is efficient and accurate in assessing the sustainability of the RIS-assisted WPT network. Furthermore, the key design for large-scale wireless networks is also provided in their work.

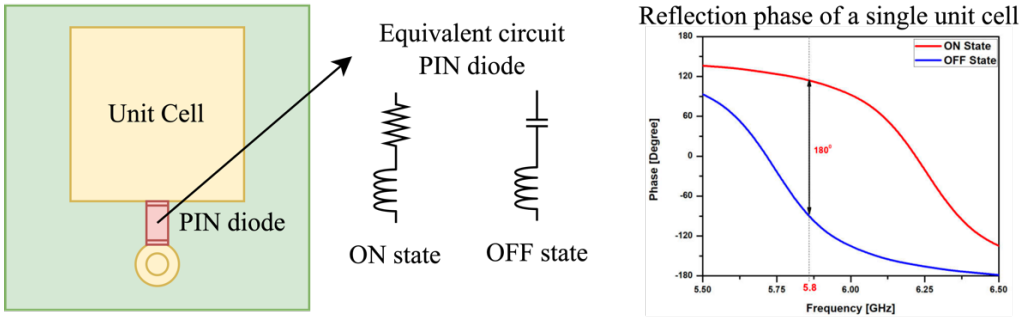

Figure 2. Basic structure and the reflection phase of a single unit cell (Tran et al., 2019)

In order to configure the RIS accordingly, each unit cell inside the RIS needs to be adjusted independently. One of the methods is to control the reflection phase of the unit cell by using a PIN diode (Tran et al., 2019). The PIN diode is used to set a unit cell in two different states. As shown in Figure 2, during the on state, the PIN diode is equivalent to the circuit of the resistor and inductor in series. On the other hand, during the off state, the PIN diode is equivalent to the circuit of a capacitor and inductor in series. Thus, by providing a control signal to the PIN diode, we can change the impedance of the PIN diode, which affects the reflection phase of the unit cell. Both the on and off states let the unit cell reflect the incoming EM signal at identical reflection magnitudes. However, the reflected EM signal has a 180° phase difference between the on and off states.

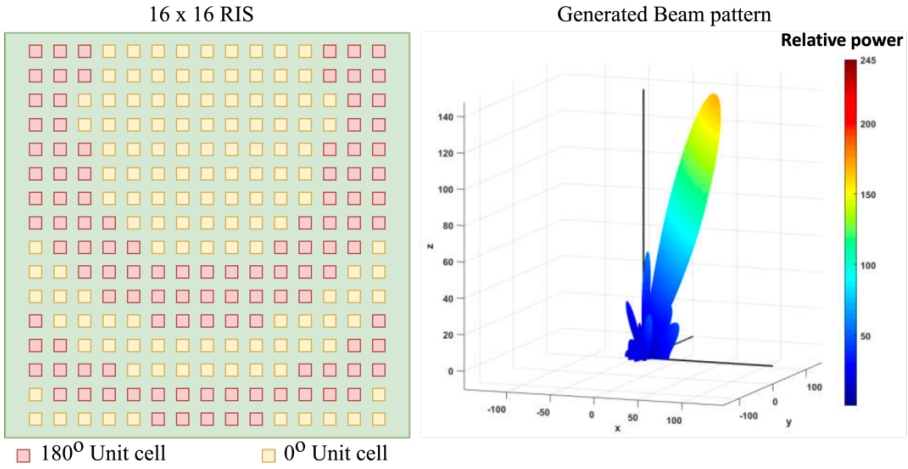

Figure 2. Optimal ON/OFF pattern for 30° direction in 1-bit RIS and the generated beam pattern (Tran et al., 2019)

Furthermore, Tran et al. (2019) implemented the ON/OFF coding pattern algorithm. This pattern is generated by several steps, starting with training, channel estimation, optimal phase calculation, phase quantization, and finally, generating the optimal ON/OFF pattern. As shown in Figure 3, this pattern is generated for a RIS with 1-bit unit cells. Thus, a certain number of unit cells are set to reflect the signal at the 0° reflection phase, and the remaining are set at 180°. By generating this pattern, the reflected signal can be directed toward the desired location.

This paper studies the RIS-assisted RF WPT for the IoT system. A comprehensive system model, including the spatial and EM propagation models of RIS-assisted RF WPT, is presented in this work. The proposed system is evaluated at the center frequency of 920 MHz, which complies with the frequency band for the IoT network (e.g., LoRA and NB-IOT). This study provides a performance evaluation of multiple RIS configurations for the RF WPT in the IoT system.

3. System Model

3.1. *Spatial Model*

As shown in Figure 4, the system model uses three-dimensional Cartesian and spherical coordinate systems to define the spatial model. The proposed system has an RF WPT transmitter device, an RF WPT receiver device, an obstacle, and an RIS device. Each RF WPT transmitter and receiver device has a single antenna. All of the elements in this system are stationary at their locations. In this system, the obstacle completely blocks the direct WPT propagation path between the RF WPT transmitter and receiver devices; thus, no direct WPT signal is received from the transmitter.

The RIS device in this system is configured as a rectangular planar array arranged in the x-y plane. The center point of the RIS device is located at the origin of the coordinate system. The RF WPT transmitter and receiver devices are deployed in the far-field region of the RIS device toward the positive z-axis. The RIS device consists

of unit cells, where denotes the number of columns and denotes the number of rows. The notation indexes the th column of the unit cell, where increases toward the positive x-axis. Meanwhile, the th row of the unit cell is indexed by the notation, which increases toward the positive y-axis. Henceforth, the unit cell at the th column and th row in the RIS can be denoted by unit cell. The distance between two center points of neighboring unit cells in the x and y directions is denoted by and, respectively.

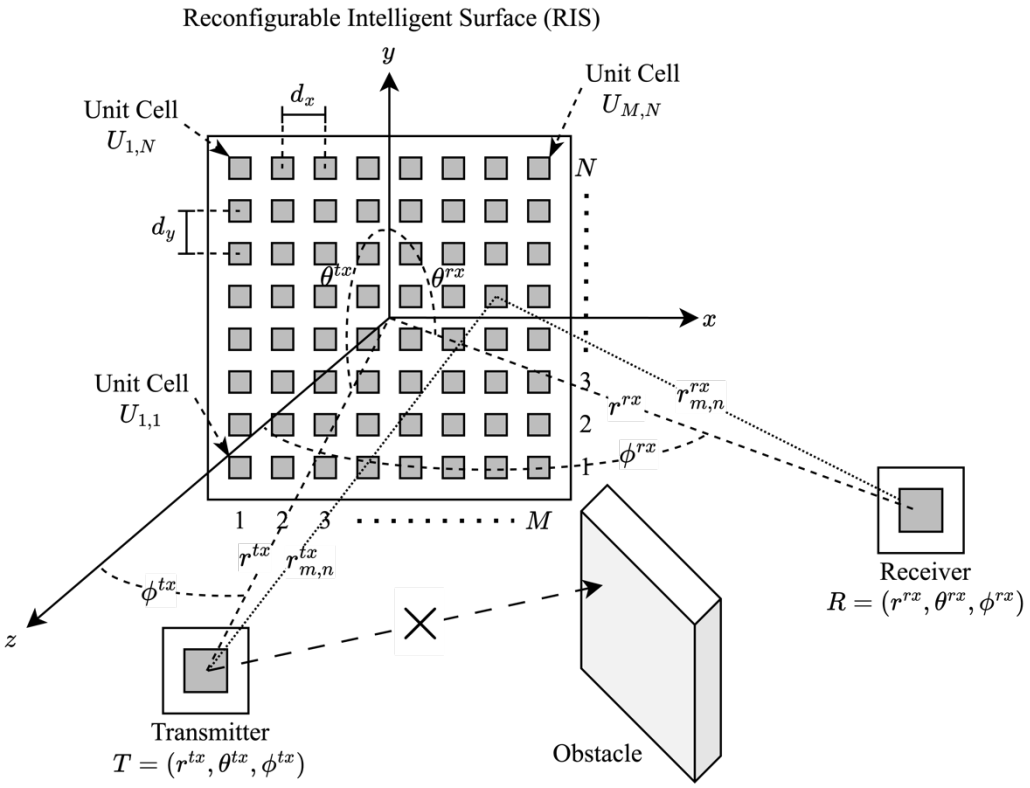

Figure 3. System Model RIS-Assisted RF WPT

The system model uses tuple $(x, y, z)^T$ to denote the location of the unit cell in the Cartesian coordinate system, where x, y, and z are the location in the x, y, and z direction, respectively. The location of unit cell (m, n) can be denoted by $U_{(m,n)} = \left(x^U_{m,n}, y^U_{m,n}, z^U_{m,n}\right)^T$, where $x^U_{m,n}$, $y^U_{m,n}$, and $z^U_{m,n}$ denote the location of unit cell (m, n) in the x, y, and z direction, respectively. The location of unit cell (m, n) can be calculated as

$$x^U_{m,n} = \left(m - \frac{M+1}{2}\right) \times d_x \quad \text{.....1)}$$

$$y^U_{m,n} = \left(n - \frac{N+1}{2}\right) \times d_y \quad \text{.....2)}$$

$$z^U_{m,n} = 0 \quad \text{.....3)}$$

The system model uses tuple $(r, \theta, \phi)^T$ to denote the location of the RF WPT devices in the spherical coordinate system, where r, θ, and ϕ are the radius, elevation, and azimuth, respectively. The transmitter device is located at $T = (r^{tx}, \theta^{tx}, \phi^{tx})^T$, where r^{tx}, θ^{tx}, and ϕ^{tx} denote the radius, elevation, and the azimuth of the transmitter, respectively. The location of the transmitter in the Cartesian coordinate system can be calculated as

$$x^{tx} = r^{tx} \sin\theta^{tx} \sin\phi^{tx} \quad \text{.....4)}$$

$$y^{tx} = r^{tx} \cos\theta^{tx} \quad \text{.....5)}$$

$$z^{tx} = r^{tx} \sin\theta^{tx} \cos\phi^{tx} \quad \text{.....6)}$$

where x^{tx}, y^{tx}, and z^{tx} denote the location of the transmitter in x, y, and z direction, respectively. Thus, with a slight abuse of notation, the location of the transmitter device in the Cartesian coordinate system is $T = (x^{tx}, y^{tx}, z^{tx})^T$.

Meanwhile, the receiver device is located at $R = (r^{rx}, \theta^{rx}, \phi^{rx})^T$, where r^{rx}, θ^{rx}, and ϕ^{rx} denote the radius, elevation, and the azimuth of the receiver, respectively. Similarly, the location of the receiver in the Cartesian coordinate system can be calculated as

$$x^{rx} = r^{rx} \sin\theta^{rx} \sin\phi^{rx} \quad \text{.....7)}$$

$$y^{rx} = r^{rx} \cos\theta^{rx} \quad \text{.....8)}$$

$$z^{rx} = r^{rx} \sin\theta^{rx} \cos\phi^{rx} \quad \text{.....9)}$$

where x^{rx}, y^{rx}, and z^{rx} denote the location of the receiver in x, y, and z direction, respectively. Thus, with a slight abuse of notation, the location of the receiver device in the Cartesian coordiate system is $R = (x^{rx}, y^{rx}, z^{rx})^T$.

Distance between the transmitter device and unit cell (m, n) is denoted by $r_{m,n}^{tx}$ and can be calculated as

$$r_{m,n}^{tx} = \sqrt{\left(x^{tx} - x_{m,n}^{U}\right)^2 + \left(y^{tx} - y_{m,n}^{U}\right)^2 + \left(z^{tx} - z_{m,n}^{U}\right)^2} \quad \text{.....10)}$$

Meanwhile, distance between the receiver device and unit cell (m, n) is denoted by $r_{m,n}^{rx}$ and can be calculated as

$$r_{m,n}^{rx} = \sqrt{\left(x^{rx} - x_{m,n}^{U}\right)^2 + \left(y^{rx} - y_{m,n}^{U}\right)^2 + \left(z^{rx} - z_{m,n}^{U}\right)^2} \quad \text{.....11)}$$

3.2. *RIS-Assisted RF WPT Model*

In this system, the transmitter device transmits RF WPT at the transmit power of P^{tx}. Let Ω denote the radiation resistance of the RF WPT antenna. The transmit signal (i.e., transmit voltage) at the transmitter device can be denoted as s^{tx}. Thus, the transmit power at the transmitter device can be calculated as

$$P^{tx} = \frac{|s^{tx}|^2}{2\Omega} \quad \text{.....12)}$$

Transmit signal s^{tx} is a complex cosine phasor of signal across the transmit antenna. The transmit signal s^{tx} can be obtained as $s^{tx} = \sqrt{2\Omega P^{tx}}$.

Figure 3 shows that the RIS device provides an alternative propagation path between the transmitter and the receiver. In this case, the received signal at the receiver is excited by the combination of the reflected signal by the unit cells in the RIS device. Note that the RF WPT system requires significantly more power than the communication system. The nonline of sight (NLOS) signal reflected by the random scatterer in the environment is significantly small compared to the LOS signal. In this case, the random channel model describing the multipath NLOS channel in the scattering environment can be neglected. Henceforth, the matrix of the received signal can be defined in a matrix equation form as

$$\boldsymbol{S^{rx}} = \boldsymbol{H^{tx}} \boldsymbol{\Gamma} \boldsymbol{H^{rx}} s^{tx} \quad \text{.....13)}$$

where $\boldsymbol{H^{tx}}$ is the matrix of propagation channel of the transmitter to unit cell (m, n), $\boldsymbol{H^{rx}}$ is the matrix of propagation channel of unit cell (m, n) to the receiver, $\boldsymbol{\Gamma}$ is the reflection coefficient matrix of the RIS device, and s^{tx} is the transmit signal from the transmitter.

In (13), Matrix $\boldsymbol{H^{tx}}$ is a $N \times M$ matrix, where $\boldsymbol{H^{tx}}$ can be defined as

$$\boldsymbol{H^{tx}} = \begin{bmatrix} h_{1,N}^{tx} & \cdots & h_{M,N}^{tx} \\ \vdots & \ddots & \vdots \\ h_{1,1}^{tx} & \cdots & h_{M,1}^{tx} \end{bmatrix} \quad \text{.....14)}$$

where $h_{m,n}^{tx}$ is the propagation channel of the transmitter to unit cell (m, n). According to (Balanis WILEY, 2016), the propagation channel of the transmitter to unit cell (m, n) can be defined in terms of distance by

$$h_{m,n}^{tx} = \frac{\lambda\sqrt{G^{tx}G^{U}}}{4\pi r_{m,n}^{tx}} exp\left(-j\frac{2\pi}{\lambda}r_{m,n}^{tx}\right) \quad ..15)$$

where λ is the free space wavelength of the RF WPT signal, G^{tx} is the gain of the transmitter antenna, and G^{U} is the gain of the unit cells. The gain for all unit cells in the RIS device is assumed to be uniform. Meanwhile, matrix $\boldsymbol{H^{rx}}$ is a $N \times M$ matrix, where $\boldsymbol{H^{rx}}$ can be defined as

$$\boldsymbol{H^{rx}} = \begin{bmatrix} h_{1,N}^{rx} & \cdots & h_{M,N}^{rx} \\ \vdots & \ddots & \vdots \\ h_{1,1}^{rx} & \cdots & h_{M,1}^{rx} \end{bmatrix} \quad ..16)$$

where $h_{m,n}^{rx}$ is the propagation channel of the unit cell (m,n) to the receiver given in term of distance by

$$h_{m,n}^{rx} = \frac{\lambda\sqrt{G^{U}G^{rx}}}{4\pi r_{m,n}^{rx}} exp\left(-j\frac{2\pi}{\lambda}r_{m,n}^{rx}\right) \quad .17)$$

where G^{rx} is the gain of the receiver antenna.

3.3. *RIS Control Model*

In (13), the matrix of reflection coefficient $\boldsymbol{\Gamma}$ is a $M \times N$ matrix, such that

$$\boldsymbol{\Gamma} = \begin{bmatrix} \Gamma_{1,N} & \cdots & \Gamma_{1,1} \\ \vdots & \ddots & \vdots \\ \Gamma_{M,N} & \cdots & \Gamma_{M,1} \end{bmatrix} \quad ...18)$$

where $\Gamma_{m,n}$ is the reflection coefficient of unit cell (m,n). Reflection coefficient $\Gamma_{m,n}$ can be obtained as

$$\Gamma_{m,n} = exp(j\omega)\, exp\left(-j\frac{2\pi}{\lambda}\beta U_{m,n}\right) \quad .19)$$

In (19), the phase and the direction of the RIS reflected wave can be control by ω and β, respectively (Tran et al., 2022b). In this case, to optimize the power transfer efficiency, the direction of the reflected beam needs to be directed toward the location of the receiver, that is (θ^{rx}, ϕ^{rx}). Henceforth, the β for the optimal power transfer can be set as

$$\beta = (sin\,\theta^{rx}\, sin\,\phi^{rx}, cos\,\theta^{rx}, sin\,\theta^{rx}\, cos\,\phi^{rx}) \quad .20)$$

3.4. *Total Receive Power Model*

In (13), the matrix of received signal $\boldsymbol{S^{rx}}$ is a $N \times M$ matrix, given by

$$\boldsymbol{S^{rx}} = \begin{bmatrix} s_{1,N}^{rx} & \cdots & s_{M,N}^{rx} \\ \vdots & \ddots & \vdots \\ s_{1,1}^{rx} & \cdots & s_{M,1}^{rx} \end{bmatrix} \quad .21)$$

where $s_{m,n}^{rx}$ is the received signal reflected by unit cell (m,n). The total received signal can be obtained by the combination of all the elements of matrix $\boldsymbol{S^{rx}}$, such that

$$s^{rx} = \sum_{n=1}^{N}\sum_{m=1}^{M} s_{m,n}^{rx} \quad ...22)$$

Total receive signal s^{rx} is a complex cosine phasor of signal across the receive antenna. Henceforth, the total receive power at the receiver device can be calculated as

$$P^{rx} = \frac{|s^{rx}|^2}{2\Omega} \quad .23)$$

From transmit power and received power defined in (12) and (23), the power transfer efficiency can be calculated as

$$\epsilon = \frac{P^{rx}}{P^{tx}} \times 100\% \quad .24)$$

4. Simulation Setup

The proposed RIS-assisted RF WPT system is simulated in MATLAB. The simulation consists of a transmitter, receiver, and RIS device, where all devices are fixed at their location. The transmitter device is constantly transmitting power at a constant level. The RIS device is configured as a rectangular planar array arranged in the x-y plane. In this simulation, the RIS optimally directs the reflected beam to the receiver. The initial simulation parameter of the proposed RIS-assisted RF WPT system is given in Table 1.

Table 1. Initial simulation parameter of RIS-assisted RF WPT

Parameters	Notation in Model	Values
Number of Transmitter antenna		1
Number of Receiver antenna		1
Number of RIS columns	M	16
Number of RIS rows	N	16
Location of Transmitter	$T = (x^{tx}, y^{tx}, z^{tx})^T$	$(-1, 0, 1)^T$
Location of Receiver	$R = (x^{rx}, y^{rx}, z^{rx})^T$	$(1, 0, 1)^T$
Location of RIS device		$(0, 0, 0)^T$
Frequency of RF WPT		920 MHz
Distance between unit cell in x direction	d_x	0.1629 Meter
Distance between unit cell in y direction	d_y	0.1629 Meter
Quantization stage of unit cell		2
Transmit Power	P^{tx}	1 Watt

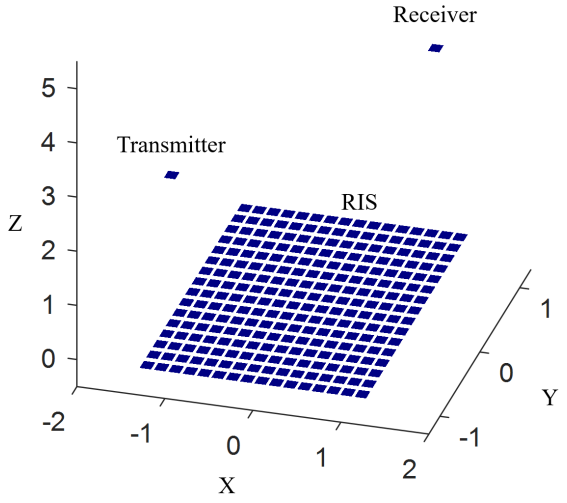

Figure 5. The initial location of unit cells, transmitter, and receiver in the MATLAB simulation

In the initial simulation setup, each unit cell is set as a one-bit unit cell capable of controlling the reflection phase by a 180-degree phase difference for each bit stage (i.e., quantization state = 2). All of the unit cells in the RIS device are assumed to fully reflect the incoming signal from the transmitter without any signal being lost or absorbed. The distance between two center points of neighboring unit cells is equal to the half wavelength of the RF WPT signal. The noise level is assumed to be far less than the transmit power. Thus, the noise can be neglected. The initial location of unit cells, transmitter, and receiver in the MATLAB simulation is illustrated in Figure 5.

5. Evaluation Result and Discussion

This section evaluates the RIS's performance for the RF WPT in the IoT system. By default, the simulation setup is set following the parameters shown in Table 1. However, at every test, certain simulation parameters are varied to study how they affect the system.

In the first simulation, the effect of physical distance on the performance of RIS-assisted RF WPT is studied. This simulation is performed by three different tests varying the distance of the transmitter and receiver device toward the RIS device. In the first test, the transmitter remains in its initial position (i.e.,. The z-position of the receiver is then increased from 1 to 15 meters. On the other hand, the second test is performed by increasing the z-position of the transmitter. At the same time, the receiver remains in its initial position (i.e.,. Meanwhile, the third test is done by simultaneously increasing the z-position of both the transmitter and receiver from 1 to 15 meters. At every z-position, the received power is measured. The results of the tests are shown in Figure 6.

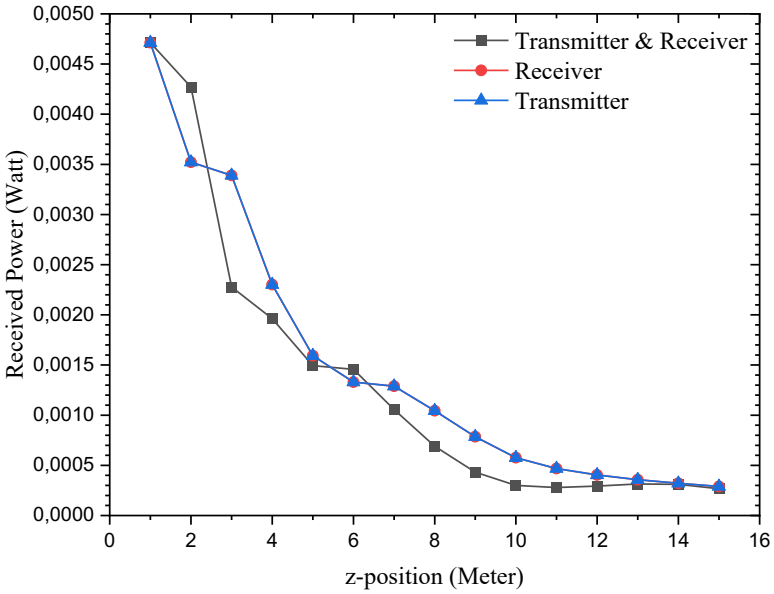

Figure 4. Received power measured at various z-position

In Figure 6, the results of the first and second tests are shown by the red and blue lines, respectively. These results are identical regardless of which device is moved further from the RIS device. At a distance of 2 meters, the measured received power is 0,00471 W. The measured receiving power decreases as the device moves further from the RIS. The receive is measured at 0,00028W at 15 meters. Meanwhile, when the transmitter and the receiver are simultaneously moved further from the RIS, the received power is lower than when only the transmitter or receiver is moved. The measured receive power is 0,0047W at 2 meters and 0,00026W at 15 meters.

These results show that the received power reduces as the radius of the RIS device increases. The propagation channels given in (15) and (17) are affected by the radius distance of the transmitter or the receiver to the unit cells. Hence, the radius distance greatly affects the received power. From the first simulation, the power transfer efficiency can be calculated by (24). The calculated power transfer efficiency based on various distances is shown in Table 2. Within a 1 meter distance, the proposed system can achieve a power transfer efficiency of 0.47%. Meanwhile, at 15 meters, the system achieves a power transfer efficiency of 0.02%. Although the system can only achieve such a low power transfer efficiency rate, this result shows that the RIS device can provide an

alternative propagation path to the system. Thus, the RF WPT can be performed with the assistance of an RIS device.

Table 2. Power transfer efficiency

z-position	ϵ when Receiver Move	ϵ when Transmitter Move	ϵ when Transmitter & Receiver Move
1	0,4714%	0,4714%	0,4714%
3	0,3390%	0,3390%	0,2278%
5	0,1594%	0,1594%	0,1494%
7	0,1289%	0,1289%	0,1057%
9	0,0786%	0,0786%	0,0432%
11	0,0468%	0,0468%	0,0279%
13	0,0358%	0,0357%	0,0314%
15	0,0290%	0,0290%	0,0267%

A similar trend to the first simulation result can be seen in the experiment result of RF WPT for the IoT system performed by Choi et al. (2019). Their RF WPT experiment was performed from a multi-antenna power beacon to a single-antenna receiver at 920 MHz, which resembles the portion of our setup from the RIS to the receiver. The difference is that their signal source is directly from the power beacon, and high-resolution phase modification results in a sharper beam pattern. Their RF WPT experiment result shows that the received power suffers as the physical distance increases. At the indoor test, their power transfer efficiency was measured at 13% at a 3-meter distance and reduced to 6% at a 5-meter distance. This means that approximately 54% of power efficiency was lost with only 2 meters of additional distance. Compared to our result when the receiver moved, the power transfer efficiency was recorded at 0,3390% at 3 meters and 0,1594% at 5 meters. Our result shows that approximately 53% of power efficiency was lost with 2 meters of additional distance. Our result is slightly better since the experiment performed by Choi et al. (2019) was performed in a non-ideal setup. Moreover, if we compare our result with the result obtained by Tran et al. (2019), who experimented with the RIS-aided WPT at 5.8 GHz, we can see that approximately 87% of power efficiency was lost with an additional 2 meters of distance from 1 to 3 meters. The comparison of these results can be seen in Table 3.

Table 3. Comparison of RF WPT test in proposed work and previous work

Reference	Power transfer technology	Operating Frequency	Power transfer efficiency	Calculated Efficiency lost with additional 2 meters distance
Choi et al. (2019)	Phase antenna Array	920 MHz	13% at 3 meters 6% at 5 meters	54%
Tran et al., (2019)	RIS	5,8 GHz	1,5% at 1 meter 0,2% at 3 meters	87%
Our work	RIS	920 MHz	0,3390% at 3 meters 0,1594% at 5 meters	53%

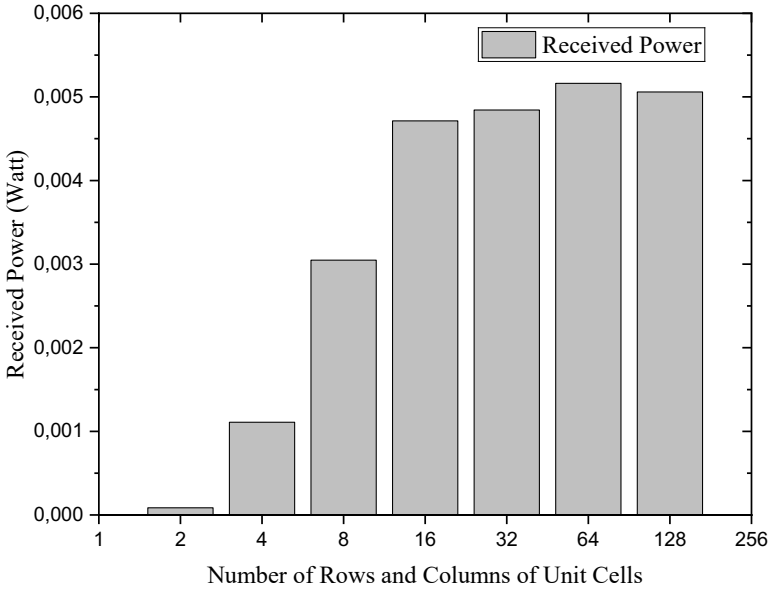

Figure 5. Received power measured by various RIS size

In the second simulation, we study how the total number of unit cells affects the performance of RF WPT. In this simulation, the number of RIS columns and rows (i.e., and)) is increased simultaneously. The transmitter and the receiver remain in their initial positions. Only the size of the RIS is increased. The result of this simulation is shown in Figure 7.

Figure 7 shows that the number of unit cells affects the total receiver power. When the columns and rows of the unit cell are set at 2, the received power is measured at 0.00086W. The received power increases to 0,0011W when the columns and rows are increased to 4. The received power keeps increasing to 0,0030W and 0,0047W when the number of columns and rows is set at 8 and 16 simultaneously. When the number of columns and rows reaches higher than 16, only a small amount of received power increment is obtained, with received power measured around 0,005W.

The reflected beam generated by the RIS device becomes sharper as the number of unit cells increases. With a small number of unit cells, the reflected beam is not sharp enough to be focused on the receiver location, resulting in lower receiving power. As the number of unit cells increases, the reflected beam becomes sharper, thus resulting in higher concentrated power at the receiver. However, increasing unit cell size after a certain number of unit cells is ineffective due to small power increments, especially for a single antenna receiver.

Compared to the work done by Choi et al. (2019), an additional number of antennas for RF WPT experimented in their work shows that the power transfer efficiency is increased by approximately 0.5% for every 8 additional antennas added to the power beacon. The power efficiency increases linearly from 1 antenna to 56 antennas. However, when the number of antennas increased to more than 56, we could see that the power efficiency growth was lower than before. Only about 0.2% additional power efficiency is obtained when the number of antennas is increased from 56 to 64. We can see a similar trend in our result when the number of unit cells is increased to 32 antennas and higher. We can see that after a certain number of unit cells, only a small amount of additional power can be received.

6. Conclusion

In this study, it has been verified that the RIS device is capable of assisting the RF WPT in the IoT system when the obstacle completely blocks the direct power transmission. This can be seen by the simulation results showing the various receive power measurements at the receiver when the radius distance of the RF WPT device is varied. This study also investigated the performance of the RF WPT with various RIS sizes. Based on the simulation results, the RIS size affects the reflected beam signal, thus resulting in the amount of power received.

To optimize the utilization of RIS for the RF WPT system, the distance between the RIS device and the RF WPT devices must be considered carefully since it greatly affects the received power and power transfer efficiency. Even though RIS is considered cheaper to build than a phase array, the RIS size needs to be selected carefully since the significantly large number of unit cells does not show advantages to the RF WPT system, rather increasing the complexity and physical size.

7. Acknowledgments

This research activity is supported through RIIM Kompetisi funding from the Indonesia Endowment Fund for Education Agency, the Ministry of Finance of the Republic of Indonesia and the National Research and Innovation Agency of Indonesia according to contract number 205/IV/KS/11/2023 and 369/SAM4/PPM/2023.

We also thank Telkom University and the University Center of Excellence for Intelligent Sensing-IoT, Telkom University for supporting this research activity.

References

Aziz, A. A., Putra, A. E., Kim, D. I., & Choi, K. W. (2022). Drone-Based Sensor Information Gathering System With Beam-Rotation Forward-Scattering Communications and Wireless Power Transfer. *IEEE Internet of Things Journal*, *9*(13), 11227–11247. https://doi.org/10.1109/JIOT.2021.3128532

Balanis WILEY, C. A. (2016). *Antenna Theory Analysis and Design Fourth Edition*. www.wiley.com.

Cha, S. H., Jeong, C., & Lim, S. H. (2018). Simultaneous wireless information and power transfer for internet of things sensor networks. *IEEE Internet of Things Journal*, *5*(4), 2829–2843. https://doi.org/10.1109/JIOT.2018.2825334

Choi, K. W., Ginting, L., Aziz, A. A., Setiawan, D., Park, J. H., Hwang, S. I., Kang, D. S., Chung, M. Y., & Kim, D. I. (2019). Toward Realization of Long-Range Wireless-Powered Sensor Networks. *IEEE Wireless Communications*, *26*(4). https://doi.org/10.1109/MWC.2019.1800475

Gong, S., Lu, X., Hoang, D. T., Niyato, D., Shu, L., Kim, D. I., & Liang, Y. C. (2020). Toward Smart Wireless Communications via Intelligent Reflecting Surfaces: A Contemporary Survey. *IEEE Communications Surveys and Tutorials*, *22*(4), 2283–2314. https://doi.org/10.1109/COMST.2020.3004197

Keskilammi, M. (2004). *Importance of application specific antennas on passive long-range RFID system performance*. [Doctoral dissertation, Tampere University of Technology]

Lu, X., Wang, P., Niyato, D., Kim, D. I., & Han, Z. (2015). Wireless networks with rf energy harvesting: A contemporary survey. *IEEE Communications Surveys and Tutorials*, *17*(2), 757–789. https://doi.org/10.1109/COMST.2014.2368999

Mohjazi, L., Muhaidat, S., Abbasi, Q. H., Imran, M. A., Dobre, O. A., & Renzo, M. Di. (2022). Battery Recharging Time Models for Reconfigurable Intelligent Surfaces-Assisted Wireless Power Transfer Systems. *IEEE Transactions on Green Communications and Networking*, *6*(2), 1173–1185. https://doi.org/10.1109/TGCN.2021.3120834

Nusrat, T., Roy, S., Lotfi-Neyestanak, A. A., & Noghanian, S. (2023). Far-Field Wireless Power Transfer for the Internet of Things. *Electronics (Switzerland)*, *12*(1). https://doi.org/10.3390/electronics12010207

Pan, C., Ren, H., Wang, K., Kolb, J. F., Elkashlan, M., Chen, M., Di Renzo, M., Hao, Y., Wang, J., Swindlehurst, A. L., You, X., & Hanzo, L. (2021). Reconfigurable Intelligent Surfaces for 6G Systems: Principles, Applications, and Research Directions. *IEEE Communications Magazine*, *59*(6), 14–20. https://doi.org/10.1109/MCOM.001.2001076

Rana, M. M., Xiang, W., Wang, E., Li, X., & Choi, B. J. (2018). Internet of Things Infrastructure for Wireless Power Transfer Systems. *IEEE Access*, *6*, 19295–19303. https://doi.org/10.1109/ACCESS.2018.2795803

Sahu, K. N. (2014). Study of RF Propagation Losses in Homogeneous Brick and Concrete Walls using Analytical Frequency Dependent Models. *IOSR Journal of Electronics and Communication Engineering*, *9*, 58–66. https://api.semanticscholar.org/CorpusID:26382706

Selvaraj, M., Vijay, R., Anbazhagan, R., & Rengarajan, A. (2023). Reconfigurable Metasurface: Enabling Tunable Reflection in 6G Wireless Communications. *Sensors (Basel, Switzerland)*, *23*(22). https://doi.org/10.3390/s23229166

Taylor, C. D., Gutierrez, S. J., Langdon, S. L., & Murphy, K. L. (1999). On the Propagation of RF into a Building Constructed of Cinder Block Over the Frequency Range 200 MHz to 3 GHz. In *IEEE Transactions on Electromagnetic Compatibility* (Vol. 41, Issue 1).

Taylor, C. D., Gutierrez, S. J., Langdon, S. L., Murphy, K. L., & Walton, W. A. (1997). Measurement of RF Propagation into Concrete Structures over the Frequency Range 100 MHZ to 3 GHz. In J. H. Reed, T. S. Rappaport, & B. D. Woerner (Eds.), *Wireless Personal Communications: Advances in Coverage and Capacity* (pp. 131–144). Springer US. https://doi.org/10.1007/978-1-4615-6237-5_13

Tran, N. M., Amri, M. M., Park, J. H., Hwang, S. Il, Kim, D. I., & Choi, K. W. (2019). A novel coding metasurface for wireless power transfer applications. *Energies*, *12*(23). https://doi.org/10.3390/en12234488

Tran, N. M., Amri, M. M., Park, J. H., Kim, D. I., & Choi, K. W. (2022a). Multifocus Techniques for Reconfigurable Intelligent Surface-Aided Wireless Power Transfer: Theory to Experiment. *IEEE Internet of Things Journal*, *9*(18), 17157–17171. https://doi.org/10.1109/JIOT.2022.3195948

Tran, N. M., Amri, M. M., Park, J. H., Kim, D. I., & Choi, K. W. (2022b). Reconfigurable-Intelligent-Surface-Aided Wireless Power Transfer Systems: Analysis and Implementation. *IEEE Internet of Things Journal*, *9*(21), 21338–21356. https://doi.org/10.1109/JIOT.2022.3179691

Wu, Q., & Zhang, R. (2020). Towards Smart and Reconfigurable Environment: Intelligent Reflecting Surface Aided Wireless Network. *IEEE Communications Magazine*, *58*(1), 106–112. https://doi.org/10.1109/MCOM.001.1900107

Xie, L., Shi, Y., Hou, Y. T., & Lou, A. (2013). Wireless power transfer and applications to sensor networks. *IEEE Wireless Communications*, *20*(4), 140–145. https://doi.org/10.1109/MWC.2013.6590061

Yang, H., Cai, C., Yuan, X., & Liang, Y. (2021). RIS-aided constant-envelope beamforming for multiuser wireless power transfer: A max-min approach. *in China Communications, 18*(3)*,* 80-90. https://doi.org/10.23919/JCC.2021.03.007

Yang, H., Cao, X., Yang, F., Gao, J., Xu, S., Li, M., Chen, X., Zhao, Y., Zheng, Y., & Li, S. (2016). A programmable metasurface with dynamic polarization, scattering and focusing control. *Scientific Reports*, *6*. https://doi.org/10.1038/srep35692